Li, Be, and B production in reactions of 45–100 MeV protons with ^{12}C: Astrophysical implications*

C. T. Roche,[†] R. G. Clark,[‡] G. J. Mathews, and V. E. Viola, Jr.

Cyclotron Laboratory and Department of Chemistry, University of Maryland, College Park, Maryland 20742

(Received 2 February 1976)

Cross sections for the production of mass 6 to 11 isobars from proton spallation of carbon targets have been measured at bombarding energies of 45, 55, 60, 65, 75, and 100 MeV. Isotopic cross sections for Li and Be have also been measured at 100 MeV. The excitation functions for these reactions have been used to test theories of Li, Be, and B nucleosynthesis. The measured abundance ratios for ^{11}B/^{10}B and B/Be can be reproduced using the experimental cross sections and astrophysical models which propose LiBeB synthesis in nuclear reactions well above the threshold energy. In order to obtain the natural ^{7}Li/^{6}Li, Li/Be, and Li/B abundance ratios, however, it is concluded that a substantial amount of ^{7}Li must be synthesized via some lower energy mechanism.

NUCLEAR REACTIONS ^{12}C(p, HI); HI Mass numbers A = 6, 7, 9, 10, and 11; E = 45, 55, 60, 65, 75, 100 MeV; HI Li and Be at 100 MeV; measured σ, $\sigma(\theta)$, and $\sigma(E)$; astrophysical implications of the data are discussed.

I. INTRODUCTION

The origin of the elements in nature is generally associated with stellar evolution.[1] As stars proceed through a sequence of hydrostatic equilibrium conditions, gravitational pressure in the stellar core generates charged particle fusion reactions between the constituent nuclei. This process of stellar nucleosynthesis is believed to be the major source of the cosmological abundances[2] of the elements carbon through iron, and also accounts for some helium. The light elements lithium, beryllium, and boron (LiBeB) are bypassed in this synthesis scheme. Because of the low binding energies of LiBeB nuclei, they are highly unstable at the temperatures and pressures encountered in stellar interiors. As a result of this instability, the calculated equilibrium concentrations of these elements within stellar cores are several orders of magnitude below their cosmic abundances.[3,4]

In order to account for the synthesis of LiBeB, nonequilibrium processes which occur in low-density astronomical environments are generally proposed.[4,5] In these settings LiBeB isotopes are produced by high-energy endoergic reactions between ^{1}H or ^{4}He and heavier nuclei such as ^{12}C, ^{14}N, and ^{16}O. The observation that the LiBeB/CNO ratio $\approx$ 1 in cosmic rays, compared to the value for representative solar system material (LiBeB/CNO $\approx 10^{-6}$), strengthens this hypothesis.[6] The major theories accounting for the origin of LiBeB have recently been reviewed by Reeves[4] and Audouze and Tinsley.[5] Among the proposed nonequilibrium sources of LiBeB are (1) interaction of galactic cosmic rays with the interstellar gas,[7]

(2) reactions initiated at stellar surfaces during the early stages of evolution,[8] (3) formation in pulsating[9] or exploding stars,[10] and (4) formation during the initial stages of cosmological expansion, i.e., the big bang.[11]

In order to examine the validity of the above theories, cross-section information for the production of LiBeB from light-ion bombardment of CNO targets is necessary. Extensive ^{12}C(p, HI) cross-section data are currently available for proton bombarding energies below 45 MeV.[12,13] (Here we define HI as representing mass numbers 6–11.) Considerable data also exist above 100 MeV where the excitation functions become independent of bombarding energy.[14-18] However, for many of the ^{12}C(p, HI) product nuclei the peak of the excitation function lies in the previously unmeasured energy region from 45–100 MeV, where relative abundance calculations are sensitive to the magnitude and peak energy of the excitation functions. In this paper we present cross-section data for 45–100 MeV proton bombardments of carbon. Our results are combined with those obtained at other energies in order to test current theories of LiBeB synthesis.

II. EXPERIMENTAL PROCEDURES

The experiments were conducted at the University of Maryland 256 cm sector-focused insochronous cyclotron using proton beams of 45.0, 55.0, 60.0, 65.0, 75.0, and 100.0 MeV in energy. The optics of the beam transport system were adjusted to insure a beam energy spread of less than 0.1%. The time width of the beam packet varied between 0.5 and 1.0 ns. The beam current was monitored

by a Tomlinson 2000 automatic frequency control AFC beam current integrator and by scaling the elastically scattered protons from the carbon targets. Beam intensities of 100-200 nA were maintained during these experiments and integrated current values are known to an accuracy of 5%.

Thin targets of spectroscopically pure carbon were used in order to minimize the error resulting from excessive energy degradation and stopping of the low-energy reaction products. Elastically scattered proton spectra, in combination with a combustion analysis of representative targets, demonstrated that less than 5% oxygen and hydrogen were present in the targets. The thicknesses of the two targets used in these experiments were determined by weight to be 113 $\mu g/cm^2$ and 50 $\mu g/cm^2$. An uncertainty of $\pm 10\%$, which includes effects of local nonuniformity, is assigned to these thicknesses and is included in the total errors.

The $^{12}C(p, HI)$ reaction products were identified with a ΔE-E surface barrier detector telescope which combined both time-of-flight (TOF) and particle-identification (PI) techniques. The reaction product masses were determined by the TOF technique. For the problem of LiBeB nucleosynthesis mass identification is a sufficient condition for

cross-section determinations since on an astrophysical time scale ($\sim 10^9$ yr), all of the particle-stable reaction products are either β stable (^6Li, ^7Li, ^9Be, ^{10}B, and ^{11}B), or undergo β decay to these isotopes. The one exception is 0.127 sec ^9C, which decays to particle-unstable ^9B. The yield of ^9C from high-energy breakup of ^{12}C has been shown to be quite low[18] relative to the particle-stable products of mass 9, and hence is assumed to be negligible here. Cross-section information for individual nuclides was obtained from the particle identification data. In these experiments the PI technique
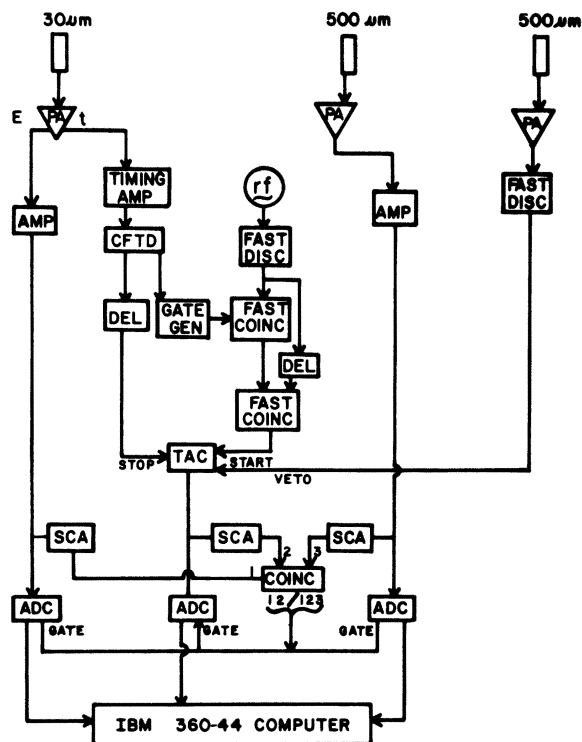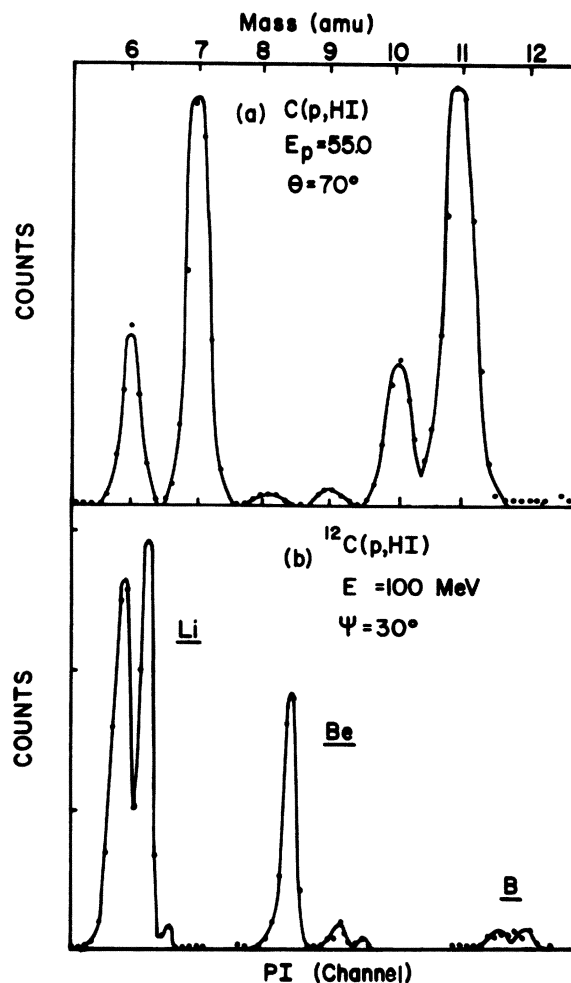

FIG. 2(a). Mass spectrum for $A = 6$ to 11 isobars formed in reactions between 55 MeV protons and carbon. Measurement performed at an angle of 70° with respect to the beam axis. Solid lines represent Gaussian fitting routine used to extract cross section information. Low energy cutoffs are listed in Table I. (b). PI spectrum for Li, Be, and B isotopes which penetrate the 30 μm detector; observed in reactions between 100 MeV protons and carbon, observed at an angle of 30° with respect to the beam.

FIG. 1. Schematic of electronics used in these experiments.

was limited by the fact that the product energy spectra are concentrated at energies below 10 MeV and hence many fragments do not penetrate the first element of the telescope. For this reason useful data could only be obtained for Li and Be isotopes.

The detector telescope was located at distances of 35–65 cm from the target in the various experiments. Our optimum experimental arrangement consisted of three silicon surface barrier detectors of thicknesses 30, 500, and 500 μm, respectively. (Some experiments at lower energies utilized a 75 μm-200 μm telescope.) The fragment time of flight relative to the cyclotron rf was measured with the 30 μm detector. Use of a thin detector for the first element of the telescope minimized the timing signal rise time. The timing pulse was further improved by overbiasing the detector by 50% and with the use of a specially designed pre-amplifier[19] located 6 cm from the detector. A low-energy cutoff in the TOF energy spectra resulted due to the presence of hydrogen and helium ions originating from the succeeding cyclotron rf burst. In order to minimize this wraparound effect, a

relatively thin (30 μm) detector was chosen as the first element in the telescope. By selecting only TOF events which stopped in the 30 μm detector in the data analysis, it was possible to reduce significantly the uncertainties due to this effect. Table I gives the experimental low-energy cutoffs in the TOF spectra for representative product ions. The second detector (500 μm) was sufficiently thick to stop the most energetic ^{6}Li produced, and ^{6}He ions up to 40 MeV in energy. (Errors due to undetected ^{6}He are negligible because the energy spectra are peaked at low energies and the total yield ratio for ^{6}He/^{6}Li is expected[18] to be less than $\frac{1}{10}$.) Both detectors were calibrated with α particle sources and a precision pulse generator designed to duplicate the heavy-ion signal shape. The third detector acted as an event veto for energetic light particles produced in these reactions (p,d,t,τ,α).

The particle identification information was used to extrapolate production ratios for the various isotopes. This is of particular interest in the case of 2.5×10^6 yr Be^{10}, since the abundance of this nuclide is used to infer the mean lifetime of
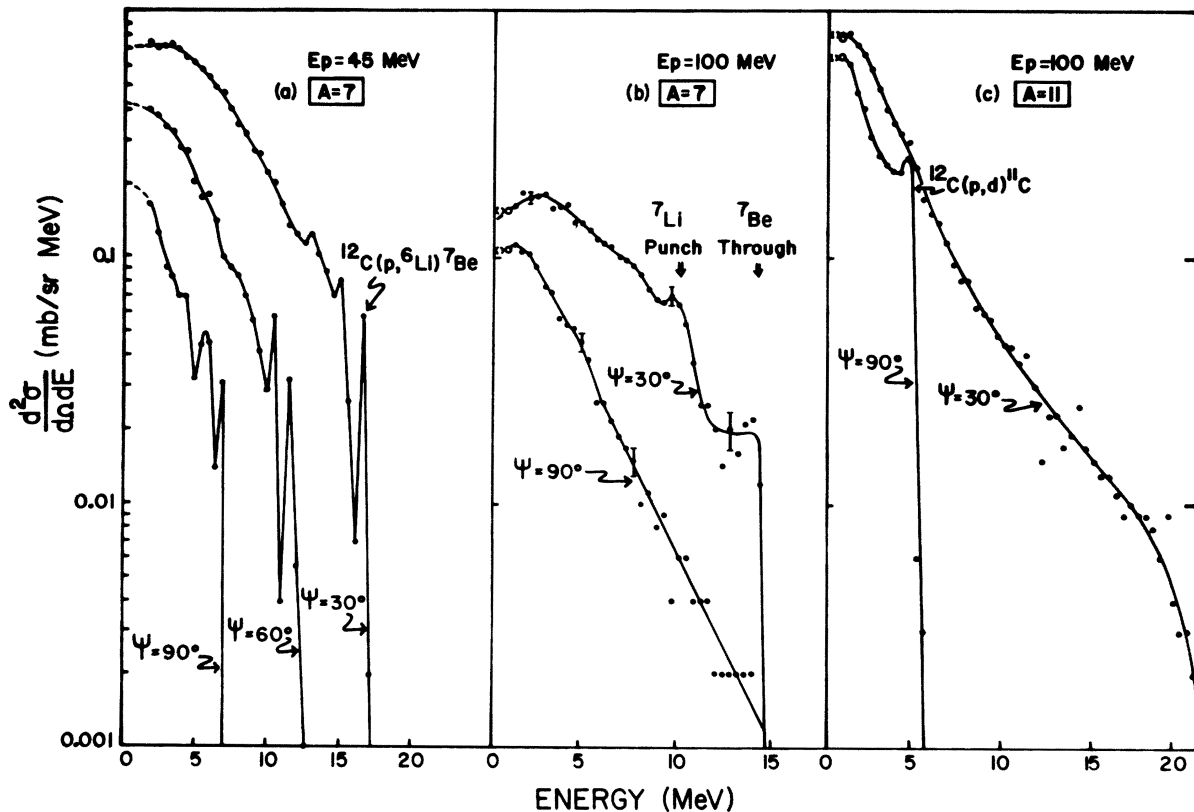

FIG. 3. Energy spectrum observed in first detector element for fragments produced in the following reactions: (a) ^{12}C(45 MeV $p, A = 7$); (b) ^{12}C(100 MeV $p, A = 7$); and (c) ^{12}C(100 MeV $p, A = 11$). Open circles represent data taken from portion of energy spectrum in which wraparound effects occur.

TABLE I. Representative low-energy limits to spal-
lation product energy spectra for time-of-flight measure-
ments.

E_p (MeV)	Cutoff energies (MeV)	
	$A = 6$	$A = 11$
45	1.8	3.4
55	2.2	4.1
60	2.4	4.4
65	3.4	6.2
75	2.9	5.4
100	0.8	1.1

cosmic radiation within the galaxy. Individual iso-
tope cross sections also have been important in
understanding the mechanism by which heavy pro-
ducts are generated from light target nuclei
in spallation reactions.

A schematic of the electronics used in these ex-
periments is shown in Fig. 1. The system consist-
ed of two linear amplification circuits, a timing
circuit, and a system veto. A pulse in the first
detector larger than 500 keV triggered the timing
circuit, measuring the time difference between
the detected event and the preceding rf signal. The
fast logic signal derived from the detector pro-
vided the stop signal for the time-to-amplitude
converter (TAC), and opened a coincidence gate
for the rf pulse, thus providing the TAC start. By
adjusting the relative delays of the stop and gate
signals we could position the signals of interest
within the linear region of the TAC. A signal in
the third detector generated an anticoincidence
gate for the TAC and stopped further processing
of an event. The energy signals from the first
two detectors and the relative time signals were
digitized and fed to an IBM 360-44 computer. The
data were stored in an event-by-event mode on
magnetic tape and sampled by an on-line acquisi-
tion code to provide interactive energy, mass,
and charge displays.

Mass and charge identification were determined
by the algorithms

$$\text{mass} = A + B(E + \Delta E)(T_0 - \text{TAC})^2 ,\qquad (1)$$

$$\text{charge} = C + D[(0.6\Delta E + E)^{0.173} - E^{0.173}]^{1/2} .\qquad (2)$$

The quantities A, B, T_0, C, and D are parameters
which were empirically determined from the data;
ΔE is the energy deposited in the 30 μm detector;
E is the energy in the 500 μm detector, and TAC
is proportional to the particle flight time. Repre-
sentative mass and particle spectra for the pro-
ducts, as determined from Eqs. (1) and (2), are
shown in Figs. 2(a) and 2(b), respectively. For
Li and Be isotopes satisfactory separation is ob-
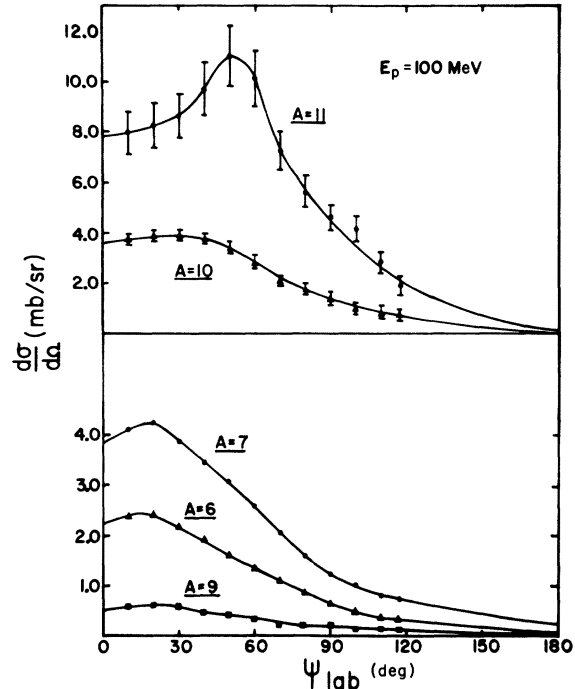tained in the PI spectra; however, in order to ob-

FIG. 4. Laboratory angular distributions for $A = 6$, 7,
9, 10, and 11 fragments produced in reactions of
100 MeV protons with carbon.

tain total cross sections, it was necessary to in-
corporate the systematics of the TOF energy
spectra into the analysis. For B isotopes too
small a fraction of the products penetrated the 30
μm detector to permit useful isotope separation.
In the time-of-flight data a mass resolution full
width at half maximum (FWHM) of approximately
0.4 amu was achieved. Projection onto the energy
axis gives a set of mass-separated energy spectra,
examples of which are shown in Fig. 3. At low
energies, a number of two-body final states (e.g.,
mass 7 at 45 MeV) are clearly defined in the data;
these become much less significant at the higher
energies, except for the (p,d) reaction. A low-
energy cutoff in $d^2\sigma/d\Omega dE$ was observed in all
spectra due to the previously mentioned effects
(~0.1 MeV/nucleon at $E_p = 100$ MeV). The 100 MeV
experiments were designed to emphasize the low-
energy region of the product spectra and show
that these spectra become flat in the energy region
below approximately 2-3 MeV and then decrease
as zero energy is approached (Fig. 3). For data
reported here, extrapolation of the low-energy re-
gion was based upon the shape of the energy spec-
tra obtained at 100 MeV, since it is observed that
the spectral shape is not a strong function of ener-
gy. An uncertainty of one-half of this extrapolated
value is included in the error estimates. This pro-
blem was most severe for the heaviest masses

TABLE II. Total production cross sections in mb for $^{12}C(p,\mathrm{HI})$ reaction.

(MeV)	HI (Mass number)				
Energy	$A=6$	$A=7$	$A=9$	$A=10$	$A=11$
45.0	13.3±2.7	39.9±7.4	···	28.6±6.6	104.6± 2.4
55.0	13.4±2.5	35.6±6.4	2.3±0.6	23.8±5.7	81.5±20.9
60.0	14.9±2.8	34.1±6.5	···	34.5±8.0	75.9±22.4
65.0	17.6±3.5	36.2±7.1	···	36.3±8.1	80.0±18.9
75.0	13.6±2.5	29.4±5.6	2.6±0.6	27.8±5.4	76.7±14.3
100.0	10.9±1.1	21.1±2.1	2.8±0.4	22.0±2.8	67.5± 7.9
		11.5±2.6(^{7}Be)		$0.5^{+0.4}_{-0.2}$(^{10}Be)	
		9.6±2.4(^{7}Li)			

measured and is reflected in the quoted errors.

The laboratory angular distributions were measured from 10° to 117° for 100 MeV protons. These are shown in Fig. 4. For the lower energies the angular range extended from 10° to 150°. Unmeasured angles were interpolated by a Lagrangian four-point interpolation technique. Integration of the angular distributions gives the total cross section results listed in Table II. The total errors combine uncertainties in counting statistics, energy and time resolution, low-energy extrapolations, and uncertainties due to target thickness, angle, flight-path, and integrator current measurements. For the 100 MeV data values of the ^{7}Li, ^{7}Be, and ^{10}Be isotopic cross sections were derived from the PI data and are also listed in Table II. In the cross-section calculations for ^{7}Li and ^{7}Be it was assumed that the spectrum shape below the PI punch-thru energy was the same for both isotopes; i.e., identical to the gross spectrum shape for $A=7$ determined from the TOF data [see Fig. 3(b)]. The ^{10}Be spectrum shape was assumed to be equal to that for ^{9}Be. Errors were estimated from the systematics of the spectral shapes for adjacent isotopes and doubled to account for the uncertainty of the method. This error was added in quadrature to the above mentioned errors to obtain the final value. The ^{7}Be value is in agreement with that of Williams and Fulmer[20] and the ^{10}Be value is consistent with the value of 1.1 ± 0.2 mb obtained by Fontes et al. at 155 MeV.[15]

III. RESULTS AND DISCUSSION

The excitation functions shown in Fig. 5 compare the present data with lower-energy time-of-flight measurements of Ref. 12. The data are in good general agreement with both Ref. 12 and data for $A=6$ and 7 from Ref. 8. On the basis of the new data it appears that the $A=6$ and 10 excitation functions have a somewhat larger magnitude and peak at a higher energy than was originally expected.[8] All excitation functions are seen to reach

a maximum well below 100 MeV, except for ^{9}Be. Comparison of our 100 MeV cross sections with higher-energy data[15,16,18,21] in Fig. 6 indicates that the excitation functions are essentially flat beyond this energy. Again, ^{9}Be is the exception. The energy independence of these cross sections at high energies is an important factor in the theoretical interpretation of the data, since the observed cosmic ray energy spectrum extends well beyond maximum energy at which cross-section measurements can be performed (see below). Empirical calculations of Bernas et al.[8] show general agreement with the shapes and magnitudes of most of
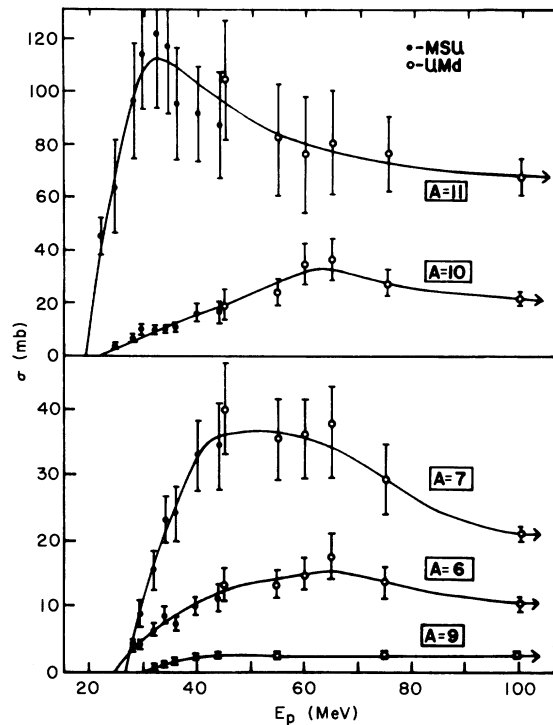

FIG. 5. Excitation functions for $E_p \leq 100$ MeV for production of $A=6$, 7, 9, 10, and 11 isobars in reactions between protons and carbon. Open points are this work and solid points are data from Ref. 12.
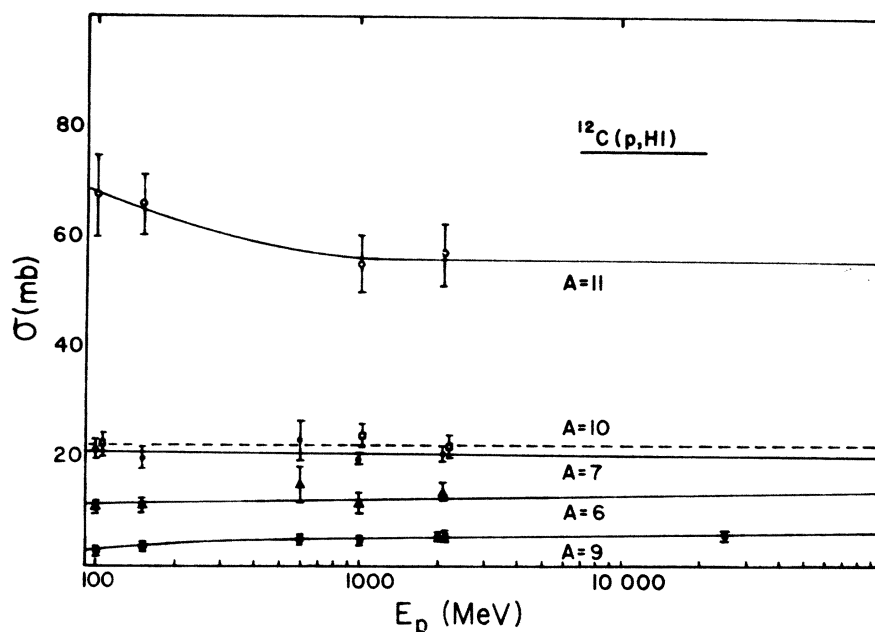
FIG. 6. Excitation functions for $E_p \geq 100$ MeV for production of $A = 6$, 7, 9, 10, and 11 isobars in reactions between protons and carbon. Data at 100 MeV are from this work, and higher energy data are from Refs. 15, 16, 18, and 21.

the measured excitation functions. This is not true for mass 11 which is underproduced in the calculations by a factor of 2 at 100 MeV. This underproduction is probably due to neglect of the large single particle contribution to the mass 11 cross section which is not considered in the calculation. Our results are in qualitative agreement with the Monte Carlo-evaporation calculations of Bertini[22] and Harp,[23] except for ^{7}Li, where the calculations are an order of magnitude too low. A more exhaustive comparison of these data with the predictions of various nuclear reaction models will be presented in a succeeding paper.

The principal test of a theory of nucleosynthesis is the degree to which it reproduces the natural isotopic and elemental abundances of the species in question. In this case we are primarily concerned with reproducing the following observed abundance ratios: ^{7}Li/^{6}Li = 12.5, ^{11}B/^{10}B = 4.1, Li/Be = 60, and B/Li = 0.2. These values are obtained from chemical analysis of meteorites and spectroscopic studies of stars and gas clouds. The values of the ^{7}Li/^{6}Li and ^{11}B/^{10}B isotopic ratios are universally accepted. However, the elemental abundances, especially that of boron, are subject to uncertainties which arise from insufficient understanding of the chemical fractionation which occurred during the condensation of the solar system. Cameron, Colgate, and Grossman[10] have argued that the B/Li ratio may be as high as 7/1. Consequently, in our discussion of

the various astrophysical models we will emphasize the Li and B isotopic ratios.

Theories of LiBeB nucleosynthesis via nonequilibrium processes can be classified as either autogenic or galactogenic. Autogenic models assume that each star generates its own LiBeB via ^{1}H or ^{4}He reactions with CNO.[8] Similarities in theLiBeB abundance ratios occurring in widely separated stars are accounted for by postulating that nucleosynthesis occurs during an early period of stellar condensation, which seems common to all stars.[24] The ^{1}H and ^{4}He particle flux is assumed to be described by a spectrum of the form $\phi(E) \propto E^{-\gamma}$, where E is the particle kinetic energy per nucleon. For the spectra observed in solar flares, $\gamma \approx 3$. Particle fluxes with this shape are very rich in low-energy projectiles. Between the threshold energy (~25 MeV) and 100 MeV the flux decreases two orders of magnitude for $\gamma = 3$. Consequently, autogenic models will be strongly influenced by low-energy resonances and by the magnitude and energy at which the excitation function peaks. The principal difficulty encountered in the autogenic models is that the energy requirements for production of the observed amounts of LiBeB are unrealistically high for stars in this phase of evolution.[25] However, Canal[26] has recently argued that the energy requirements are considerably lower than those estimated in Ref. 25.

Galactogenic theories propose that LiBeB results from the interaction of cosmic rays with in-

TABLE III. LiBeB production ratios as a function of various assumptions concerning spectra of particle flux $\phi(E)$.

Particle spectrum $\phi(E)$	Target ratio C/N/O	Production ratios			
		$^7Li/^6Li$	$^{11}B/^{10}B$	Li/Be	B/Li
Flare spectra					
$E^{-1.5}$	3/1/5	1.7	3.5	11.9	3.3
E^{-3}	3/1/5	2.4	9.5	17.4	9.5
$E^{-4.5}$	3/1/5	3.6	33.4	25.5	35.0
E^{-3} ($E > 30$ MeV)	3/1/5	1.7	3.8	8.3	3.4
Cosmic ray spectra					
$(E + M_0C^2)^{-2.6}$	3/1/5	1.4	2.0	15.3	1.2
Rigidity flux (Ref. 29)	3/1/5	1.6	2.3	14.2	1.1
Experimental values	$\cdots$	12.5	4.1	60	0.2 [a]

[a] Reference 10 proposes that this ratio may be as high as 7/1.

terstellar material.[7] Thus, these elements are inherited by a star when it condenses from the interstellar medium. The energy spectrum which characterizes the galactic cosmic ray flux is uncertain below 1 GeV and is very poorly understood below 100 MeV due to solar modulation. A spectrum shape $\phi(E) \propto (E + m_0c^2)^{-2.6}$ is usually assumed,[27] where E is the particle kinetic energy/nucleon and m_0c^2 is the nucleon rest mass. This form for $\phi(E)$ predicts a cosmic ray spectrum that bends over and becomes flat at low energies E, which is consistent with current models of solar demodulation. The ratio of low- to high-energy protons is much smaller in this type of flux than in the spectrum associated with a solar flare. Recently, several authors have proposed alternative functional forms for the galactic cosmic ray flux. Ramadurai and Biswas[28] have postulated a "Fermi" type source spectra which is equivalent to a power law in the total energy per nucleon plus a velocity term. Webber and Lezniak[29] have reexamined the primary cosmic ray proton and helium spectra in the range 10 MeV/amu to 100 GeV/amu and have proposed that the data are better fitted by a power law in the magnetic rigidity (momentum/charge). The Fermi cosmic ray spectrum is richer in low-energy protons than the $(E + m_0c^2)^{-2.6}$ representation.[11,27] In a rigidity power law spectrum the α-particle and CNO fluxes are enhanced relative to the proton flux.

We have examined several flux shapes in order to determine the effects on LiBeB production. Production rates for LiBeB are obtained from the relation

$$dN_L/dt = \sum_i N_i \sum_j \int_{E_0}^{\infty} \phi_j(E)\sigma_{ijL}(E)dE \ , \qquad (3)$$

where L represents the isotopes ^6Li, ^7Li, ^9Be, ^{10}B, and ^{11}B; N_i is the relative number of target

nuclei of type i, usually taken[30] to be H/He = 10 and C/N/O $\equiv$ 3/1/5; $\phi_j(E)$ is the incident particle flux for particle j (again with H/He = 10 and C/N/O = 3/1/5, and $\sigma_{ijL}(E)$ is the cross section for formation of product L from target i bombarded by particle j, given as a function of energy from the threshold energy E_0 to infinity. Cross-section data were based on this work and Refs. 12–18 and 21. For the rigidity power law spectrum a value of H/He = 7/1 was used. Ratios of the various isotopes and elements are calculated assuming that both the C/N/O ratio and the cosmic ray spectral shapes are time independent. In addition, the rate of LiBeB destruction due to astration is assumed to be the same for all species. In Table III the calculated production ratios of interest are tabulated for several assumptions concerning $\phi(E)$ that should bracket the real situation.

It is clear from examination of Table III that no single set of circumstances successfully reproduces the cosmic abundances for LiBeB. The most obvious conclusion to be derived from the model calculations is that under no set of realistic conditions can the $^7Li/^6Li$ and Li/Be ratios be obtained, and that the B/Li ratio is reasonable only if the enhanced boron abundance[10] is accepted. A reasonable $^{11}B/^{10}B$ ratio is obtained for $\gamma \approx 1.5-2$ and for the galactic cosmic ray flux. In order to account for the discrepancies involving lithium ratios, one must conclude that processes other than those described here are major sources of ^7Li in the universe. A number of supplemental mechanisms have been postulated that will produce additional ^7Li but no appreciable amounts of the other LiBeB isotopes.[4] Among these are: (1) formation during the "big bang"; (2) production of ^7Be during helium shell flashes in the cores of certain types of red giant stars; (3) production in supernovas; and (4) the cosmic ray reactions

$\alpha(\alpha,p)^7$Li and $\alpha(\alpha,n)^7$Be.

Recent measurements of the $\alpha + \alpha$ reaction[31] have demonstrated that there is insufficient production of mass $A = 7$ nuclides via this mechanism to account for the observed ^{7}Li/^{6}Li ratio. Also, serious problems with ^{7}Be production in He flashes exist; these are related to the transport of the ^{7}Be to the stellar surface. Jacobs et al.[13] have shown that there exist resonances in the low energy portion of the LiBe excitation functions that could provide greatly enhanced ^{7}Li/^{6}Li ratios. Such an interpretation would be consistent with a discrete energy spectrum of particles produced by a supernova shock wave. Another attractive alternative is to assume that the excess ^{7}Li is a residue of the big bang, since this is the only LiBeB product that is synthesized in any significant abundance in the big bang. This hypothesis has been previously investigated by Mitler.[11]

If one assumes that (1) approximately 80% of the ^{7}Li in nature has survived since initial production via the big bang, and (2) the remaining ^{6}Li, ^{7}Li, ^{9}Be, ^{10}B, and ^{11}B result from either galactic cosmic ray or autogenic sources, as described previously, then reasonable agreement with the experimental absolute abundances of LiBeB,[2] as well as the isotopic ratios, can be obtained. For either the galactic cosmic ray flux or $\gamma \approx 1.5-2$, the corrected ratios become: ^{7}Li/^{6}Li = 12.5 (by definition), ^{11}B/^{10}B $\approx$ 4, Li/Be $\approx$ 60, and B/Li $\approx$ 0.8. Similar satisfactory results can be found for the fluxes proposed by Refs. 28 and 29 and for a proton flux of the form ($E > 30$ MeV)

$\propto E^{-3}$ and $\phi(E \lesssim 30$ MeV$) \approx 0$, again assuming supplemental ^{7}Li production. This latter situation presumably approximates the conditions which exist in high temperature solar flares. It is interesting to note that the implied density of the universe necessary to produce the required amount of ^{7}Li in the big bang[32] is also in good agreement with the estimates of Gott et al.[33] based on other astrophysical data.

On the other hand, if the new B/Li ratio[10] of B/Li $\approx$ 7 is correct, then other mechanisms must be proposed to enhance the B/Li ratio without altering the ^{11}B/^{10}B and ^{7}Li/^{6}Li ratios. In particular, this condition appears to demand a large flux of low-energy particles. This would lead to a much more complex picture for LiBeB nucleosynthesis than has been previously postulated.

ACKNOWLEDGMENTS

*Work supported by U.S. Energy Research and Development Administration.

†Present address: Argonne National Laboratory, Argonne, Illinois.

‡Present address: Federal Energy Administration, Washington, D.C.

[1]E. M. Burbidge, G. R. Burbidge, W. A. Fowler, and F. Hoyle, Rev. Mod. Phys. 29, 547 (1957).

[2]A. G. W. Cameron, in Origin and Distribution of the Elements, edited by L. H. Aherns (Pergamon, Oxford, 1968), p. 130.

[3]S. Bashkin and D. C. Peaslee, Astrophys. J. 134, 981 (1961).

[4]H. Reeves, Annu. Rev. Astron. Astrophys. 12, 437 (1974).

[5]J. Audouze and B. Tinsley, Astrophys. J. 192, 487 (1974).

[6]V. L. Ginzberg, The Origin of Cosmic Rays (Gordon and Breach, New York, 1969).

[7]H. Reeves, W. A. Fowler, and F. Hoyle, Nature 226, 727 (1970).

[8]R. Bernas, E. Gradsztajn, H. Reeves, and E. Schatzman, Ann. Phys. (Paris) 44, 426 (1967).

[9]R. J. Talbot and W. D. Arnett, Nature 229, 150 (1971).

[10]A. G. W. Cameron, S. A. Colgate, and L. Grossman, Nature 243, 209 (1973).

[11]H. E. Mitler, Astrophys. Space Sci. 17, 186 (1972).

[12]C. N. Davids, H. W. Laumer, and S. M. Austin, Phys. Rev. C 1, 270 (1970); H. W. Laumer, S. M. Austin, L. M. Panngabean, and C. N. Davids, ibid. 8, 483 (1973).

[13]W. W. Jacobs, D. Bodansky, D. Chamberlin, and D. L. Oberg, Phys. Rev. C 9, 2134 (1974); D. Bodansky, W. W. Jacobs, and D. L. Oberg, Astrophys. J. 202, 222 (1975).

[14]M. Jung, C. Jacquot, C. Baixeras-Aiquabella, R. Schmitt, and H. Braun, Phys. Rev. C 1, 435 (1970).

[15]P. Fontes, C. Perron, J. Lestrinquez, F. Yiou, and R. Bernas, Nucl. Phys. A165, 405 (1971).

[16]R. Bernas, E. Gradsztajn, M. Epherre, R. Klapisch, and F. Yiou, Phys. Lett. 15, 147 (1965).

[17]J. Audouze, M. Epherre, and H. Reeves, Nucl. Phys. A97, 144 (1967).

[18]P. J. Lindstrom, D. E. Greiner, H. H. Heckman, B. Cork, and F. S. Bieser, Lawrence Berkeley Laboratory Report No. LBL-3650, 1975 (unpublished).

[19]J. E. Etter (unpublished).

[20]J. R. Williams and C. B. Fulmer, Phys. Rev. 154, 1005 (1967).

[21]R. Silberberg and C. H. Tsao, Naval Research Laboratory Report No. NRL-7593, 1973 (unpublished).

[22]H. Bertini (unpublished); we are indebted to Dr. S. Curtis of the Lawrence Berkeley Laboratory for providing these calculations.

[23]G. Harp (unpublished).

[24]W. K. Bonsack and J. L. Greenstein, Astrophys. J. 131, 83 (1960).

[25]C. Ryter, H. Reeves, E. Gradsztajn, and J. Audouze, Astron. Astrophys. 8, 389 (1970).

[26]R. Canal, Astrophys. J. 189, 531 (1974).

[27]M. Meneguizzi, J. Audouze, and H. Reeves, Astron. Astrophys. 15, 337 (1971).

[28]S. Ramadurai and S. Biswas, Astrophys. Space Sci. 30, 187 (1974).

[29]W. R. Webber and J. A. Lezniak, Astrophys. Space Sci. 30, 361 (1974).

[30]E. A. Muller, in *Origin and Distribution of the Elements*, edited by L. H. Aherns (Pergamon, Oxford, 1968), p. 155.

[31]C. H. King, H. H. Rossner, Sam M. Austin, W. S. Chien, G. J. Mathews, V. E. Viola, Jr., and R. G. Clark, Phys. Rev. Lett. 35, 988 (1975).

[32]R. V. Wagoner, Astrophys. J. 179, 343 (1973).

[33]J. R. Gott, III, J. E. Gunn, D. N. Schramm, and B. M. Tinsley, Astrophys. J. 194, 543 (1974).